International Journal of Research in Engineering and Science (IJRES)
ISSN (Online): 2320-9364, ISSN (Print): 2320-9356
www.ijres.org Volume 12 Issue 8 ǁ August 2024 ǁ PP. 169-181

Design and simulation of a hot-wall extruder for the production of organic-metallic frameworks

Saeed Tavangar*,Hosein Mahdavi
**Malek Ashtar University of Technology*
Corresponding Author: stavangar@mut.ac.ir

Abstract
The production of metal-organic frameworks (MOFs) on an industrial scale and in a cost-effective manner can greatly benefit this industry. In this research, one of the very innovative methods for producing metal-organic frameworks, namely the extrusion method, has been studied, and a model for extrusion has been designed. This designed model has been utilized with OpenFOAM software based on computational fluid dynamics to study the melting and compression of metal-organic frameworks within the extrusion process. Additionally, a laboratory study has been conducted to validate the developed code. In this research, 81 samples have been simulated to investigate important parameters in the extrusion of metal-organic frameworks, including the extrusion outlet diameter, the density ratio of the metal-organic frameworks, the rotation speed, and the number of screw blades, to examine their effects on the torque and power required for screw rotation, as well as the output density of the metal-organic frameworks from the extrusion. The results showed that increasing the number of blades in small diameters, such as 0.5 mm, significantly increases the flow rate, while in medium diameters, such as 1.0 mm, it has a considerable effect on the flow rate. However, in larger diameters such as 1.5 millimeters, there is a significant reduction in the output flow rate. Additionally, an increase in the compression ratio leads to a significant decrease in the output flow rate across all samples. Furthermore, increasing the diameter can enhance the flow rate up to 18 times with an acceptable density. On the other hand, the torque and power required to rotate the screw have a direct, direct, and inverse relationship with the number of blades, compression ratio, and output diameter of the extruder, respectively.

Keywords: ***Design and simulation of a hot-wall extruder for the production of organic-metallic frameworks.***

Date of Submission: 14-08-2024 Date of acceptance: 30-08-2024

I. INTRODUCTION

Metal-organic frameworks (MOFs) are microstructures that utilize an organic material as a connector between metal molecules [1]. Among the notable features of these microstructures is their very high surface-to-mass ratio; for example, one gram of MOF-5 has a surface area of 7000 square meters, making it an ideal porous medium for various applications [2]. They also exhibit high stability, flexible design, and strong resistance to thermal changes [3]. These materials can be used for carbon capture, separation of hydrogen and carbon dioxide mixtures, catalysis, drug delivery, air filtration, energy storage, chemical sensors, and water purification membranes [4-8]. Various factors, including the method, time, temperature, and pressure of synthesis, influence the acquisition of MOFs with the desired characteristics. The presence of energy for bond breaking or formation is necessary, and this phenomenon also exists in the synthesis of MOFs, as the synthesis of these compounds is based on creating bonds between organic linkers and metal oxides [9]. Generally, the temperature range used for MOF synthesis is between 15 °C and 273 °C. The main goal in synthesizing MOFs is to create specific inorganic building units without degrading the organic linker [10]. Any tool that can generate a controllable amount of heat will be suitable for MOF synthesis. For example, the heat generated can be supplied from sources such as ovens, microwave radiation, ultrasound, electric potential, and electromagnetic wave radiation [11]. The nature of the formed MOFs depends on the source or type of energy used, and their properties are contingent upon the synthesis method [12]. The application of the created MOFs depends on their primary properties, such as particle size and size distribution, and morphology. Additionally, the porosity of the synthesized MOFs is a function of the thermal energy used during synthesis as well as the heat source employed [13]. Although the synthesis of MOFs through coordinating metal clusters and organic ligands may seem straightforward, creating an optimal structure is quite challenging. Factors such as the type of solvent, pH, substituents present in the linker, and the concentration of metal ions, as well as reaction parameters (time, temperature, and pressure), affect the type of synthesized MOFs [14].

The aim of this research is to present a model that is feasible for construction and industrial application, which includes all geometric and dynamic parameters. Computational fluid dynamics (CFD) is then utilized to

study various parameters. These parameters include geometric factors such as the extrusion outlet diameter, the number of screw blades, and the compression ratio, as well as dynamic parameters like the rotational speed of the screw. The effects of these parameters on the temperature and flow rate of the MOF output from extrusion, the amount of torque, and the power required for screw rotation, along with several fluid-related parameters, have been examined. The goal is to identify the optimal conditions for producing MOF. It can be said that a significant portion of this research is novel, and to date, there has been no study, either domestically or internationally, that presents a complete model for the mechanical extrusion of MOF and the use of computational fluid dynamics in this context. In this research, the extrusion consists of two separate parts named the barrel and the screw.

II. The geometry and simulation method

The barrel is considered the outer body of the extrusion, responsible for heating the material and directing it. Figure 1 shows the designed barrel, which resembles a hollow cylindrical rod that tapers to a point at one end, with a small hole at the end for the exit of the MOF. Table 1 also presents the values for each of the geometric parameters.

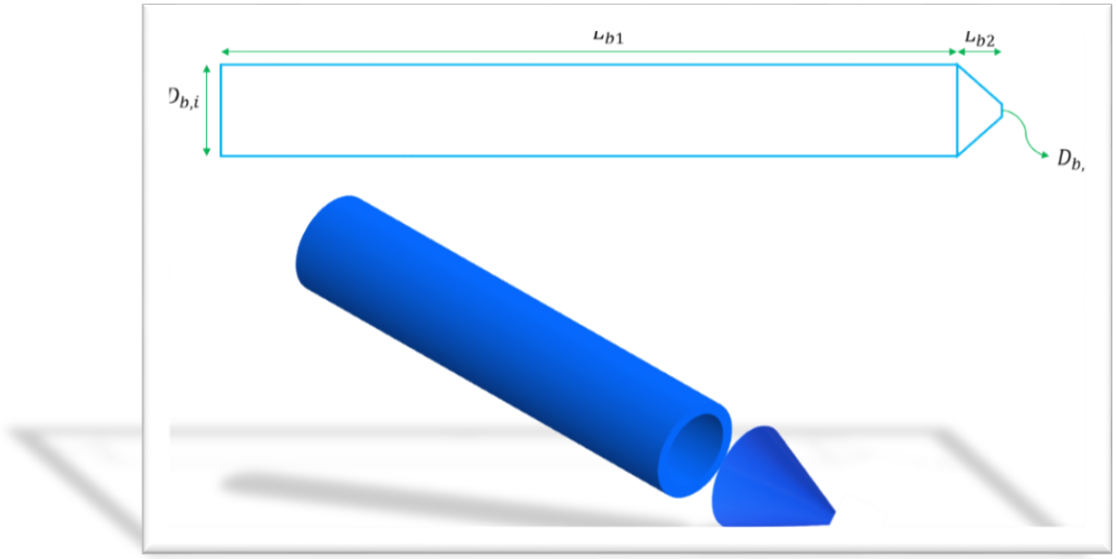

Figure 1: Barrel or extrusion body in two and three dimensions showing geometric parameters.

he other utilized engineering component is the screw, which is designed to push and compress the MOF inside the barrel. Figure 2 shows a view of the screw, which is a metal piece with blades around it that are continuously twisted at a specific angle from the beginning to the end of the metal shaft. Additionally, the screw has two zones known as the feed-melt zone and the compression zone. The first zone of the screw, located at the beginning of the extrusion process, receives the combined solid materials through a hopper. In this zone, due to the very low rotational speed of the screw, there is sufficient time for the materials to melt. After the materials have melted, they enter the second zone, which is the compression zone, where the screw compresses them while guiding them toward the extrusion outlet to obtain the MOF. In Figure 2, all the geometric parameters required for constructing the screw are shown, and Table 2 presents the values of these parameters.

Table 1: Required values of barrel geometric parameters.

Geometrical parameter	value
L_{b1}	290
L_{b2}	10
$D_{b,i}$	20.2
$D_{b,o}$	0.5, 1.0, and 1.5

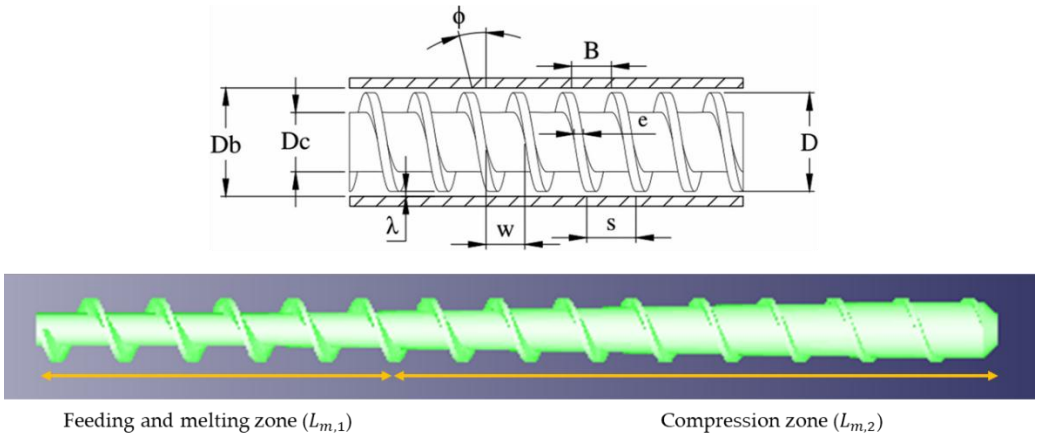

Figure 2: The designed geometry for the screw along with the geometric parameters.

Table 2: Values of geometric parameters for the screw.

definition	Value
Thread width (B)	11
Screw diameter (D)	20
Screw core diameter ($\boldsymbol{D_c}$)	10
Barrel inner diameter ($\boldsymbol{D_b}$)	20.2
Total screw length (L)	294
Feeding-Melting zone length ($\boldsymbol{L_{m1}}$)	100
Compression-zone length ($\boldsymbol{L_{m2}}$)	194
Helix angle Φ (°)	17.65
Groove depth in the feeding-zone ($\boldsymbol{h_r}$)	3
Groove depth in the metering- zone ($\boldsymbol{h_m}$)	1.2
Screw width €	12
Screw groove width *(W)*	10.2
Pitch *(S)*	1
Screw to barrel clearance ($\boldsymbol{\lambda}$)	0.1

In this process, a mixture of specified materials for the production of MOF is initially introduced into the extrusion through a hub. The material mixture consists of organic and metallic substances that have been blended together prior to injection. After injection, the mixture receives heat through the warm barrel wall to melt the organic materials, and then it enters the densification area to increase density, where metal-organic bonds are formed under high pressure. Finally, the formed MOF exits through a small nozzle at the end of the extrusion. In many transport phenomena, assumptions are made for the use of these equations, and in addition to those, assumptions have also been made for the present issue, which can be summarized as follows: Non-steady, laminar flow, compressible under pressure, non-Newtonian viscosity, heat generation due to viscosity, neglecting the effects of gravity and external forces, considering kinetic and internal energy, accounting for volumetric stress, and assuming constant thermal conductivity and specific heat capacity. As a result, the equations of mass, momentum, and energy conservation can be presented as follows:

$$\frac{d\rho}{dt} + \nabla.(\rho V) = 0 \tag{1}$$

$$\frac{D(\rho V)}{Dt} = \nabla.\sigma \tag{2}$$

$$\sigma = -pI + \tau = -pI + \mu[(\nabla.V) + (\nabla.V)^T] - \frac{2\mu}{3}(\nabla.V)I \tag{3}$$

$$\frac{D(\rho e)}{Dt} + \nabla.(\rho VV + pI) = \nabla.(k\nabla T) + \mu\Phi \tag{4}$$

$$e = \frac{1}{2}V^2 + u \tag{5}$$

$$\Phi = \tau : \nabla V \qquad (6)$$

In the above equations, V, p, e, and u represent the velocity vector, pressure, total energy, and internal energy, respectively. Additionally, the Greek symbols ρ, μ, and k denote density, viscosity, and thermal conductivity coefficient. In the momentum equation, the stress component (σ) consists of compressive and shear stresses (τ) and the volumetric strain of the element. Furthermore, in the energy equation, the effects of volumetric change and thermal loss (Φ) due to viscosity are taken into account. Moreover, the parameter e is the sum of the kinetic and internal energy of the fluid. It can also be stated that the internal energy at the melting temperature range is equal to the enthalpy of melting, and at temperatures higher and lower than the melting temperature, it is equal to the product of the specific heat capacity at constant volume and temperature. In this issue, the boundary conditions can be presented mathematically in Table 3.

Table 3: **Boundary conditions of velocity, pressure, and temperature mathematically.**

	inlet	Screw-wall	Barrel-wall	Outlet
velocity	$\nabla V = 0$	$V = \Omega r$	$V = 0$	$\boldsymbol{\nabla V = 0}$
pressure	$P = 1\ bar$	$\nabla p = 0$	$\nabla p = 0$	$\boldsymbol{P = 1\ bar}$
temperature	$T = 23\ ℃$	$\nabla T = 0$	$T = 160\ ℃$	$\boldsymbol{\nabla T = 0}$

In this study, one of the most widely used metal-organic frameworks, namely ZIF-8, has been selected for production. To produce this material, zinc carbonate $[Zn_3O_6H_{12}][Zn_2C_2O_4]$ and methylimidazole ($C_4H_6N_2$) were used in a molar ratio of 2 to 3, and no solvents were employed. In addition to the extrusion of ZIF-8, a small amount of carbon monoxide gas and water vapor is also released due to the reactions occurring within the extruder. The ligands of this compound melt at a temperature of 145 degrees Celsius, and therefore, the external surface temperature of the barrel wall is considered to be 160 degrees Celsius.

In this research, the rhoPimpleFoam solver from OpenFOAM has been developed and used to numerically solve the governing equations of the present phenomenon. Upwind and central schemes with second-order accuracy have been employed for the divergence and Laplacian terms to discretize the equations. On the other hand, the numerical solution is based on iteration, and the residuals of 10^{-5}, 10^{-4}, and 10^{-6} for velocity, temperature, and pressure have been used to stop each case. Table 4 is provided for examining and selecting the mesh based on the output flow rate, which shows that mesh 419452 can be a reasonable choice for simulating other cases.

Table 4: Independence Output from the Number of Meshes for Conditions
$CR = 9, NF = 22, \Omega = 20\ RPM, and\ D_o = 1.5\ mm$

Mesh number	Mass flow rate(gr/min)	Error[1]
52,367	18.128	+33.01
124,651	15.864	+16.39
241,325	14.251	+4.56
419,452	13.629	-
112,4981	13.523	-2.93

Figure 3 on the left and the bottom row also shows the geometry imported into OpenFOAM. All the required values for the study's screw [1] were provided, as shown in Table 5.

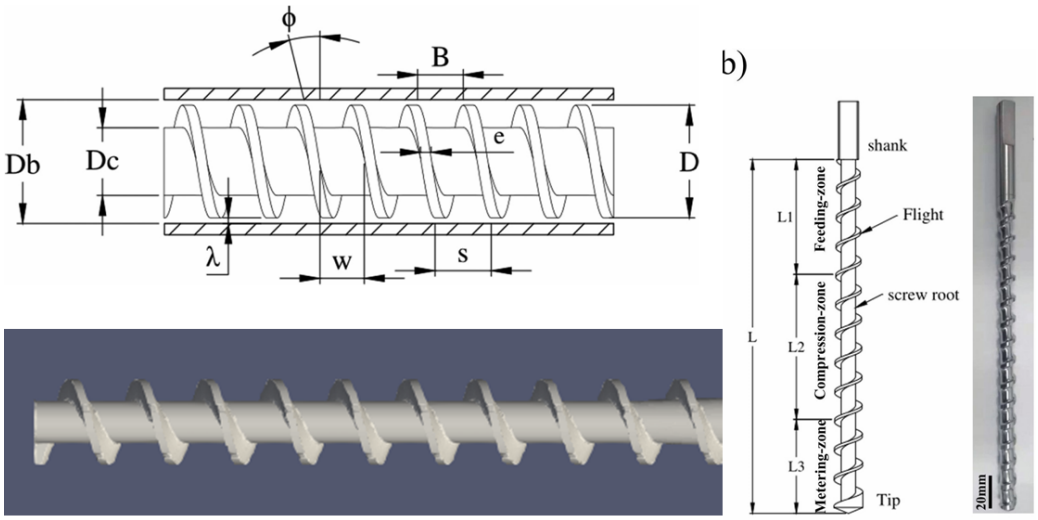

Figure 3: The designed screw along with the parameters in study [1] and the geometry imported into OpenFOAM in this research.

Table 5: Values of the parameters required for the design of the screw studied [1].

definition	Value
Thread width *B* (mm)	11
Screw diameter *D* (mm)	12
Barrel inner diameter D_b (mm)	12.2
Total screw length *L* (mm)	204
Feeding-zone length L_1 (mm)	106
Compression-zone length L_2 (mm)	53
Metering-zone length L_3 (mm)	45
Helix angle *Φ* (°)	17.65
Groove depth in the feeding-zone h_F (mm)	3
Groove depth in the metering- zone h_M (mm)	1.2
Screw width *e* (mm)	12
Screw groove width *W* (mm)	10.2
Pitch *S* (mm)	1
Screw to barrel clearance *λ* (mm)	0.1

III. Results and discussion

In the present research, several geometric and dynamic parameters that significantly affect the industrial-scale production process of MOFs have been selected, with definitions and reasons for the selection of each parameter provided below.

Screw Rotational Speed This is a dynamic parameter that regulates the rotational speed of the screw inside the fixed barrel, measured in revolutions per minute (RPM). This parameter has a significant impact on the suction rate of the input materials or the amount of MOF produced, as the angle of the screw blades is designed to direct the materials toward the outlet, and changes in rotational speed affect the material flow. Additionally, variations in rotational speed also influence the quantity of the molten mixture. In this study, the values are set at 10, 15, and 20 RPM.

Barrel Outlet Diameter This is a geometric parameter related to the barrel that, in addition to regulating the output flow rate from the extrusion process, also affects its density. The geometric shape of MOF materials can vary with compression. This parameter is set in the barrel during the meshing process in Gambit software, with values of 0.5, 1.0, and 1.5 millimeters used in this research.

Number of Screw Blades This is a geometric parameter of the screw that not only directs the materials toward the outlet but also compresses them. As explained, in part of the screw, the diameter continuously decreases, and without the blades, the materials would not move toward the outlet. This parameter is set for values of 14, 18, and 22 blades.

Density ratio: This is the last geometric parameter of the screw that is responsible for compressing or increasing the density of the MOF. In the distance L1 of the screw, the melted material only moves towards the outlet and melts, and there is no increase in density during this interval. However, in the distance L2, the central diameter

of the screw gradually increases to compress the melted material from section L1 and increase its density. This parameter is calculated as follows:

$$CR = \frac{{D_b}^2 - {D_i}^2}{{D_b}^2 - {D_o}^2} \quad (8)$$

Which indicates the ratio of the area of the space between the barrel and the screw at the beginning of the extrusion to the end of the screw. Additionally, values of 3, 6, and 9 have been chosen for this parameter.
Table 1 represents the rerun column design specification.

3.1 The effects of various parameters on the output flow rate of MOF.

It can be confidently stated that the mass flow rate of MOF output from extrusion is the most important parameter in extrusion systems, especially when the system is designed for industrial-scale dimensions. Figure 4 shows the mass flow rate in grams per minute for different numbers of blades, compression ratios, and outlet diameters at a rotational speed of 10 revolutions per minute. According to an outlet diameter of 0.5 mm, increasing the number of blades results in an increase in the mass flow rate at all three compression ratios because as the number of blades increases, the extruder's suction increases due to the proximity of the blades to each other. Increasing the number of blades from 14 to 22 at a compression ratio of 3 has resulted in a 31.2 percent increase in the mass flow rate, which is significant. Additionally, by observing the graphs at a fixed number of blades, it can be inferred that increasing the compression ratio leads to a decrease in the mass flow rate. This is because when the compression ratio increases, the molten material in the compression zone requires sufficient time to compress and exit, and this time increases with the compression ratio. Specifically, increasing the compression ratio from 3 to 9 for 14 blades has resulted in a 7.1 percent decrease in the mass flow rate. Carefully examining the graph provided for an outlet diameter of 1.0 mm, it can be seen that for all compression ratios, increasing the number of blades from 14 to 18 leads to an increase in the mass flow rate, while further increasing it to 22 has no effect on the mass flow rate. This is because increasing the number of blades beyond 18 has not been able to enhance the suction. On the other hand, at a fixed number of blades, increasing the compression ratio leads to a decrease in the mass flow rate, which can also be supported by the graph for an outlet diameter of 0.5 mm. In other words, increasing the compression ratio from 3 to 9 for 22 blades has resulted in a 21.4 percent decrease in the mass flow rate. Now, turning to the graph provided for an outlet diameter of 1.5 mm, according to this graph, increasing the number of blades at a fixed compression ratio leads to a decrease in the mass flow rate. This is because the outlet diameter has become sufficiently large, allowing the MOF to exit the extruder easily; however, adding more blades becomes a constraint for suction, and increasing the number of blades at this outlet diameter imposes negative suction on the system, which suggests that adding more blades at this outlet diameter should be avoided.

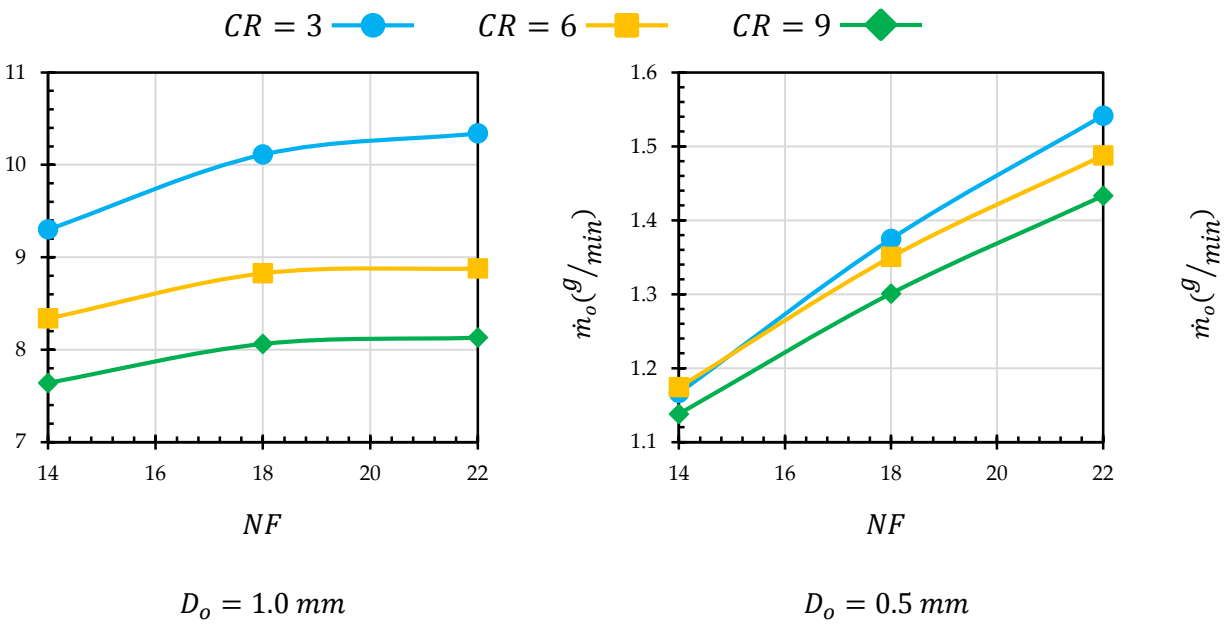

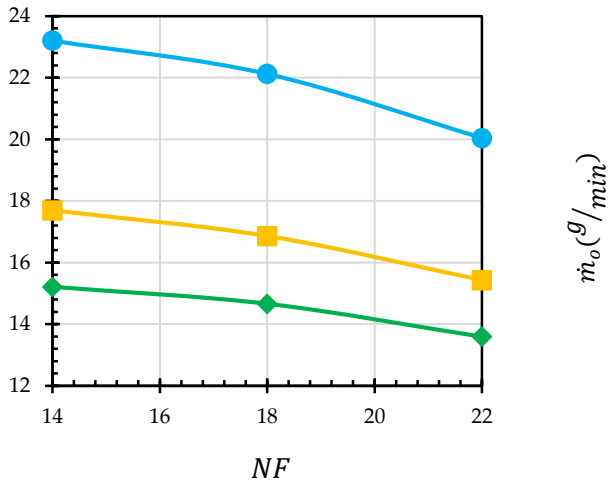

Figure4: The charts of the output mass rate of the MOF for different values of extruder outlet diameter, density ratio, and number of blades at a rotational speed of 10 revolutions per minute.

Figure 5 shows the mass flow rate of the produced MOF at an extruder output with a 1 mm diameter and a density ratio of 6, illustrating the effects of the screw rotational speed. It can be observed that increasing the number of flights at the same rotational speed slightly increases the mass flow rate; however, increasing the rotational speed from 10 to 20 revolutions per minute nearly doubles the mass flow rate output from the extruder. In other words, there is approximately a linear relationship between the screw rotational speed and the mass flow rate output.

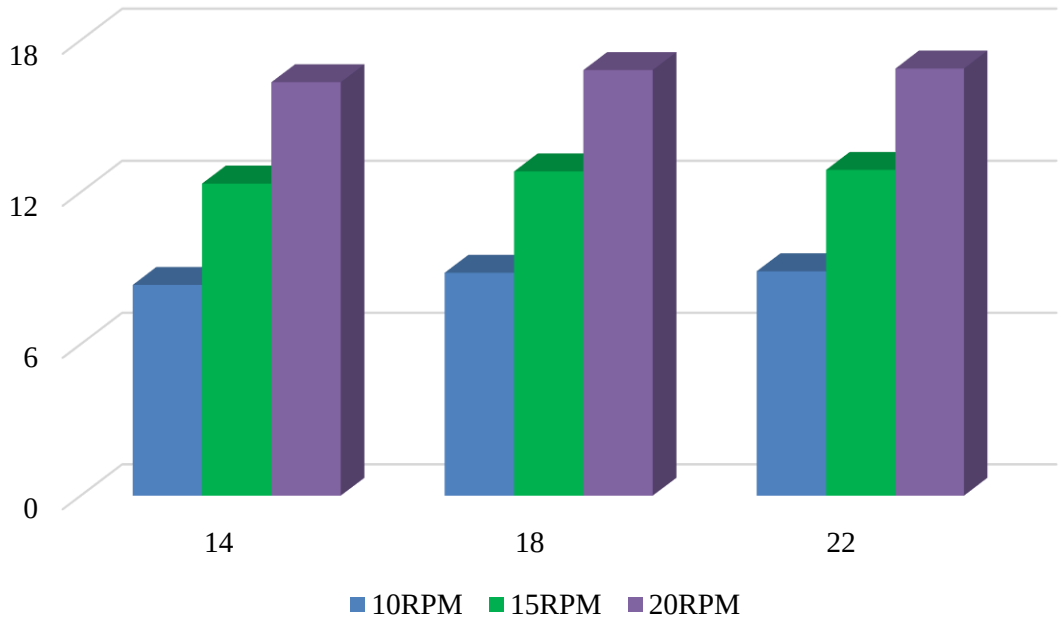

Figure 5. Graphs of the mass flow rate of MOF at an outlet diameter of 1 millimeter and a density ratio of 6 to compare the effects of screw rotational speed.

3.2 The effects of various parameters on the maximum density of MOF.

As previously demonstrated, compressing the mixture in the production of MOF materials using the extrusion method is very important. The initial average density of the material at the input was 4800, and extrusion leads to an increase in density. Figures 6 shows the maximum density curves of MOF during extrusion

for different output diameters of the extruder, density ratios, and the number of blades at a rotational speed of 10 revolutions per minute. By comparing Figures4 and 6, it can be observed that the pattern of density changes is similar to the mass flow rate of the output, as the mass flow rate is the product of speed, density, and cross-sectional area of the output. The cross-sectional area is constant, and therefore the variables are only speed and density. Consequently, according to Figure 6 and the output diameter of 0.5 mm, increasing the number of blades due to the reduction in the distance between the blades leads to an increase in density, and other arguments align with the mass flow rate of the output. It is important to note that increasing the diameter, due to reduced output resistance, results in a decrease in maximum density, such that the maximum densities for diameters of 0.5, 1.0, and 1.5 are 5330, 5220, and 5030, respectively, for 14 blades and a density ratio of 3.

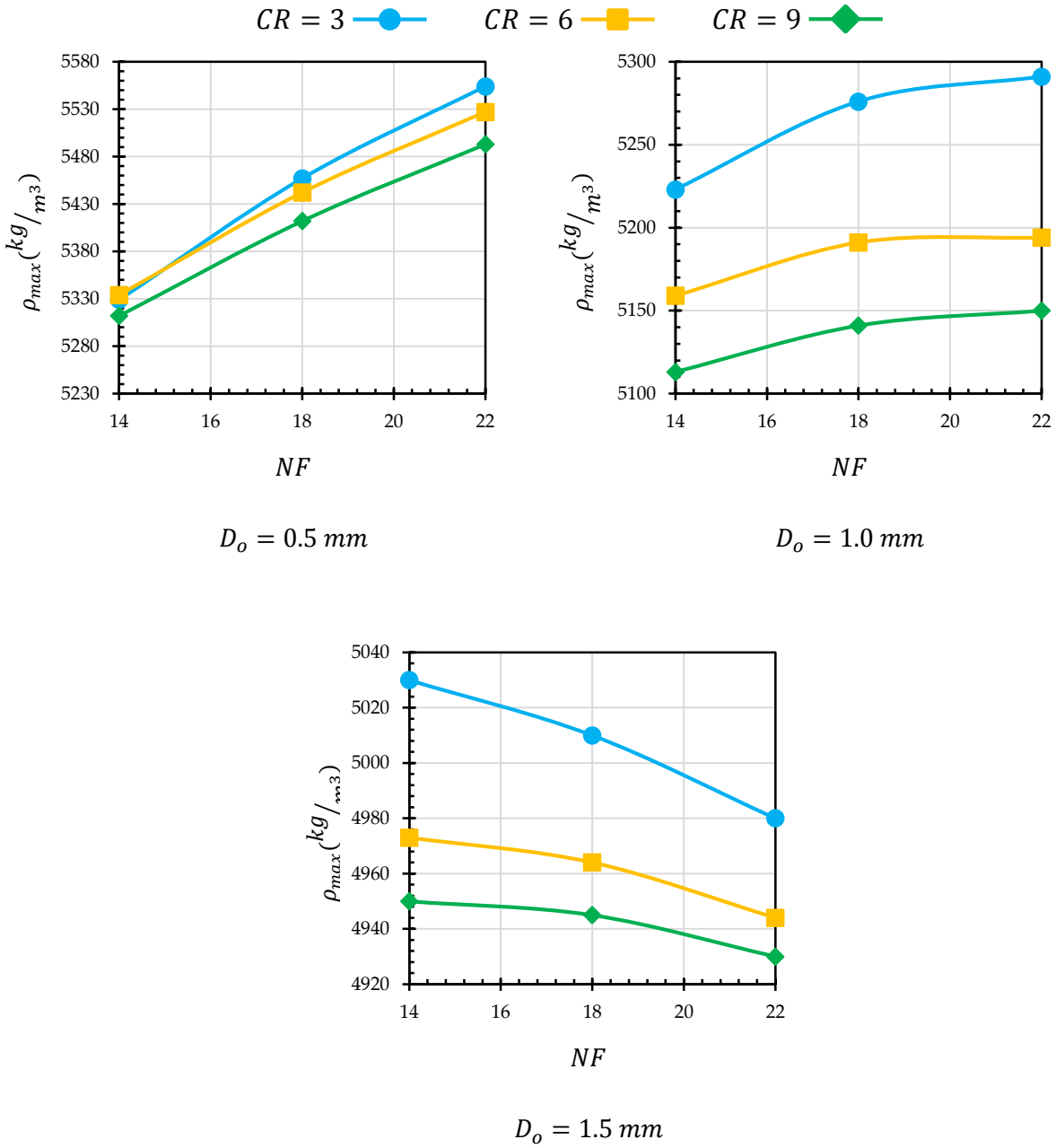

Figure 6:The maximum density charts of MOF for different values of extruder outlet diameter, compression ratio, and number of blades at a rotational speed of 10 revolutions per minute.

3.3 The effects of various parameters on the torque required for the rotation of the screw

To achieve a precise and industrial design, it is necessary to study not only the flow parameters but also the dynamic and geometric parameters in order to provide a practical and reliable model. Therefore, this section examines the torque required to rotate the screw within the extruder. Consequently, Figure 7 is presented to observe the effects of various parameters on the torque required for the screw. According to the graphs, for all

three extrusion outlet diameters, increasing the number of blades at a constant compression ratio results in an increase in the screw torque. This is because an increase in the number of blades leads to a greater contact area between the materials and the screw, which in turn results in higher angular stress and increased torque. Additionally, increasing the compression ratio with a constant number of blades also raises the required torque, as the contact area between the screw and the materials increases. As we know, torque has a direct relationship with the product of the distance from the screw's center to the surface and the angular stress applied to the screw. It can be stated that increasing the number of blades from 14 to 22 approximately increases the required torque by 12 to 17 percent. Furthermore, increasing the compression ratio from 3 to 9 increases the torque by approximately 10 to 18 percent. Moreover, the effects of the extrusion outlet diameter can also be addressed, as increasing the outlet diameter leads to a reduction in torque because MOF materials can be easily extruded at larger outlet diameters, thereby reducing the output resistance or the compressive stresses applied to the screw.

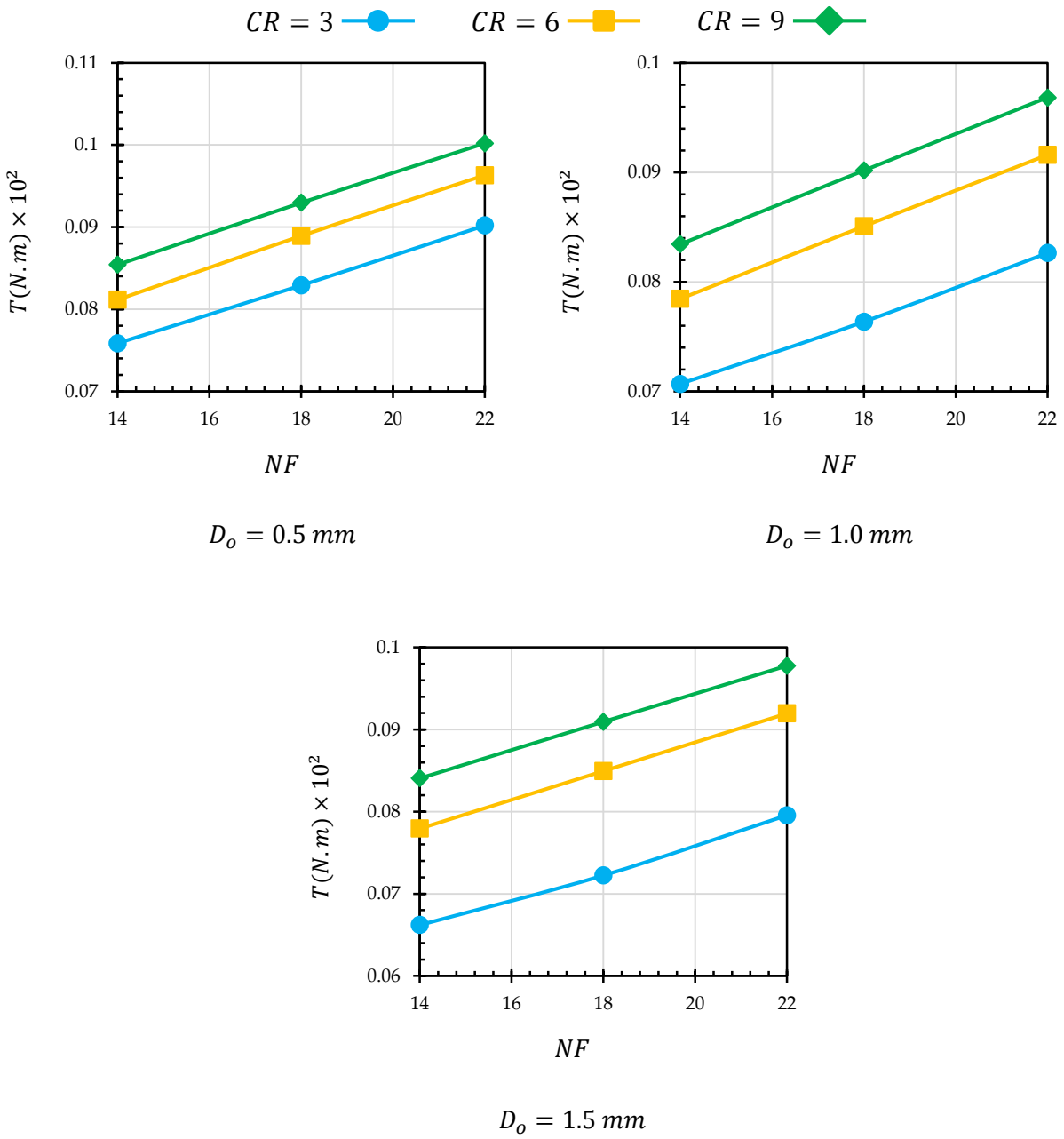

Figure7: The torque diagrams required for the screw for different output diameters of the extruder, compression ratios, and the number of flights at a rotational speed of 10 revolutions per minute.

3.4The effects of various parameters on the power required for the rotation of the screw.

Another important parameter in the post-processing of this research is the power required by a motor to rotate the screw, which is illustrated in Figure 8 to show the effects of various parameters on it. As can be seen from the graphs, the behavior of all the graphs is similar to the torque required for the screw, because according to relation 9, the required power is equal to the product of torque and the rotational speed of the screw. Additionally, the rotational speed for this curve is constant at 10 revolutions per minute. The highest torque required is observed for the maximum number of blades and the compression ratio, and of course, the smallest outlet diameter, which is equal to 86 watts.

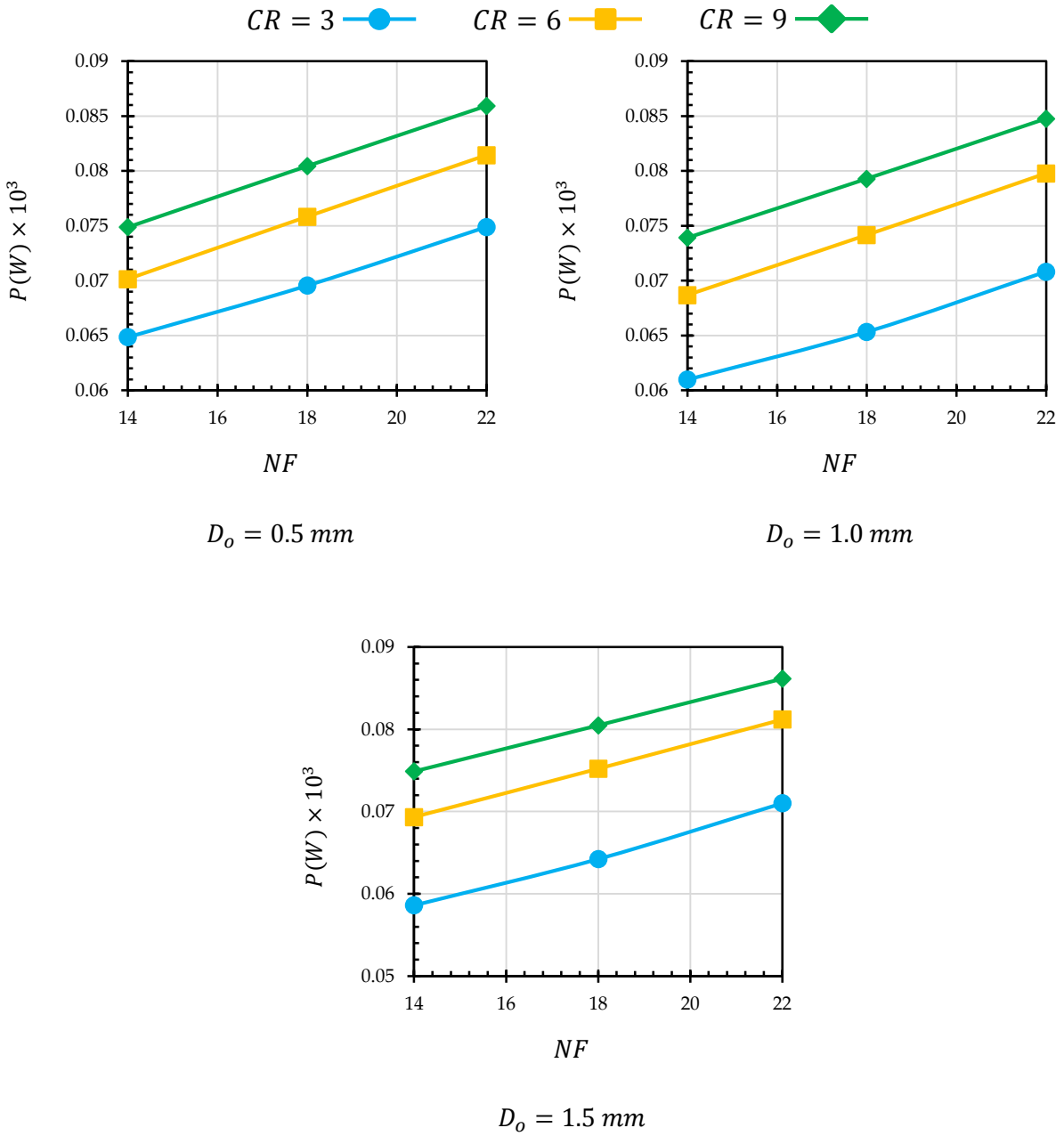

Figure8: The power requirement charts for the rotation of the screw for various output diameters of the extruder, compression ratios, and number of blades at a rotational speed of 10 revolutions per minute.

3.4 The effects of various parameters on pressure distribution.

Studying the pressure distribution and the maximum pressure points within the extrusion helps in selecting the appropriate material for the construction of the barrel and screw, as they must be able to withstand compressive and shear stresses effectively. Accordingly, Figures 9 and 10 illustrate the pressure distribution on the screw. According to both figures, the pressure in the melting zone is equal to atmospheric pressure; however, in the compression zone, pressure changes gradually until the end of the screw, indicating that the compression zone has effectively and continuously compressed the materials. Additionally, the maximum pressure for Figure 9 increases with the number of flights, but in Figure 10, the maximum pressure increases from 14 to 18 flights and does not change from 18 to 22 flights. Furthermore, by comparing these two figures, it can be concluded that the maximum pressure for the extruder with a compression ratio of 3 is greater than that of 6, as the effects of compression due to the number of flights dominate the compression ratio.

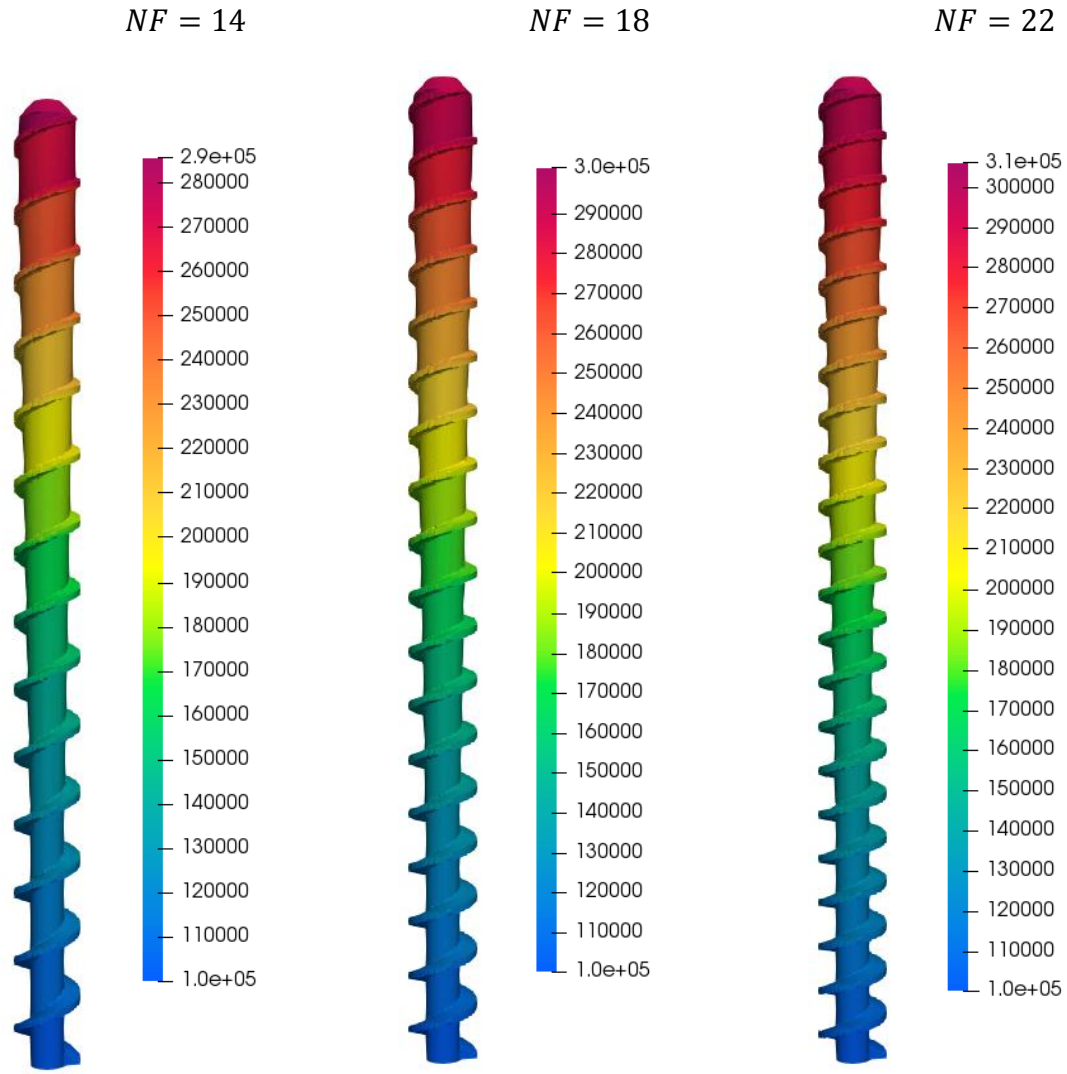

Figure 9: Pressure distribution along with the bar load for different numbers of blades at CR=3, at a rotational speed of 10 revolutions per minute and an outlet diameter of 1.0 millimeters.

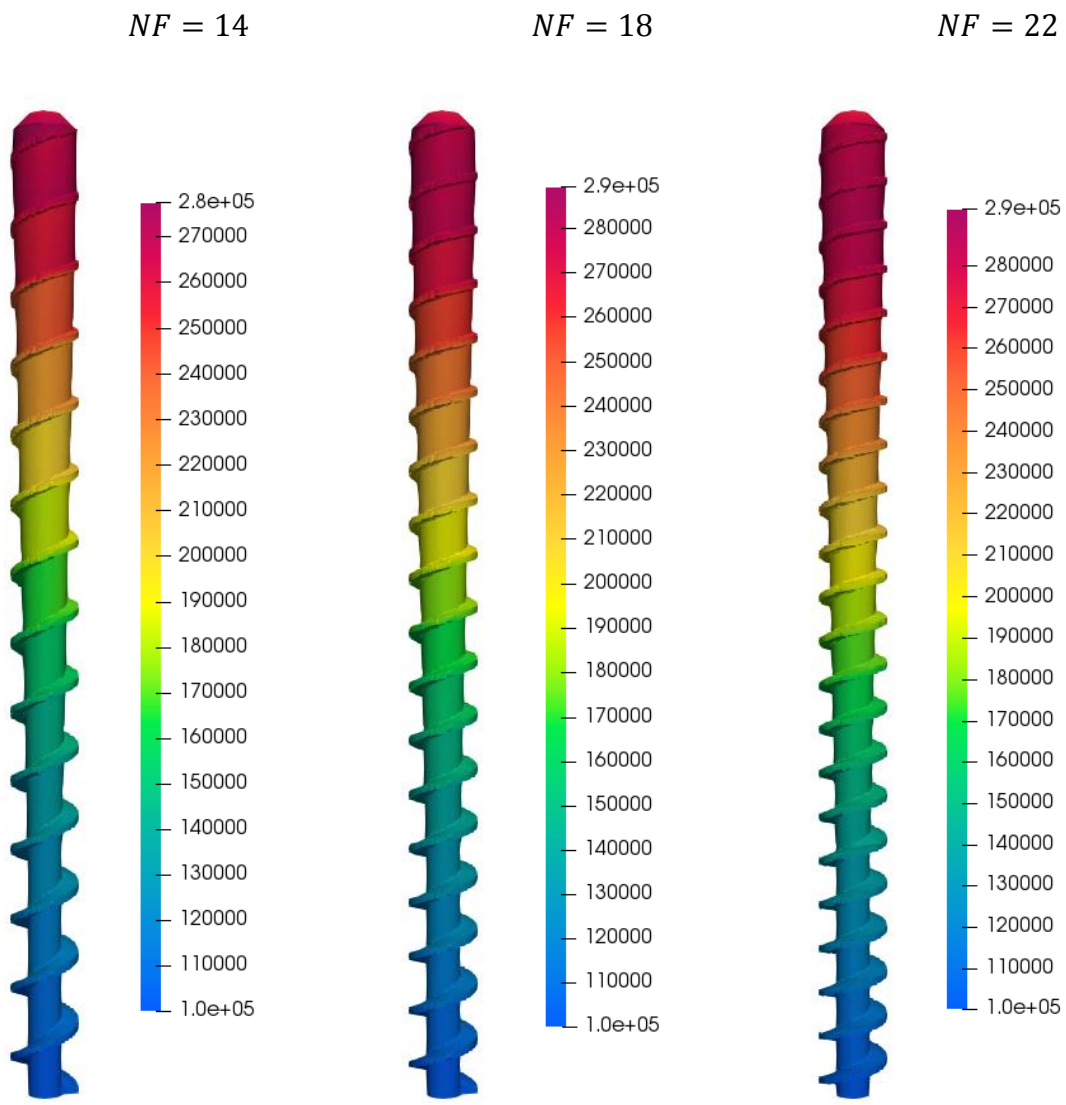

Figure10:The distribution of pressure along with the bar load for different numbers of blades at CR=6, at a rotational speed of 10 revolutions per minute and an outlet diameter of 1.0 millimeter.

IV. CONCLUSION

In this study, an extrusion system with a hot barrel and a screw was designed for the production of metal-organic frameworks (MOFs) and simulated using computational fluid dynamics and OpenFOAM software. The input variables included the diameter of the extruder outlet, the number of screw flights, and the compression ratio. Their effects on the mass flow rate of the produced MOF materials, maximum density, torque, and power required to rotate the screw, as well as the pressure distribution within the extruder, were analyzed and discussed in the results section. The results showed that increasing the number of flights significantly increases the mass flow rate at small diameters, such as 0.5 mm, while it has a considerable impact on the mass flow rate at medium diameters, such as 1.0 mm, but leads to a significant decrease in the mass flow rate at larger diameters, such as 1.5 mm. Additionally, increasing the compression ratio significantly reduces the mass flow rate in all samples. Furthermore, increasing the diameter can increase the mass flow rate by up to 18 times with acceptable density. On the other hand, the torque and power required to rotate the screw have a direct relationship with the number of flights and the compression ratio, and an inverse relationship with the extruder outlet diameter.

REFERENCES

[1]. Ding, M., Flaig, R.W., Jiang, H.L. and Yaghi, O.M., 2019. Carbon capture and conversion using metal–organic frameworks and MOF-based materials. Chemical Society Reviews, 48(10), pp.2783-2828.

[2]. Wang, H.F., Chen, L., Pang, H., Kaskel, S. and Xu, Q., 2020. MOF-derived electrocatalysts for oxygen reduction, oxygen evolution and hydrogen evolution reactions. Chemical Society Reviews, 49(5), pp.1414-1448.

[3]. Chmelik, C., 2015. Characteristic features of molecular transport in MOF ZIF-8 as revealed by IR microimaging. Microporous and Mesoporous Materials, 216, pp.138-145.

[4]. Wu, T., Liu, X., Liu, Y., Cheng, M., Liu, Z., Zeng, G., Shao, B., Liang, Q., Zhang, W. and He, Q., 2020. Application of QD-MOF composites for photocatalysis: Energy production and environmental remediation. Coordination Chemistry Reviews, 403, p.213097.

[5]. Cho, H.Y., Yang, D.A., Kim, J., Jeong, S.Y. and Ahn, W.S., 2012. CO2 adsorption and catalytic application of Co-MOF-74 synthesized by microwave heating. Catalysis Today, 185(1), pp.35-40.

[6]. Chen, L., Zhang, X., Cheng, X., Xie, Z., Kuang, Q. and Zheng, L., 2020. The function of metal–organic frameworks in the application of MOF-based composites. Nanoscale Advances, 2(7), pp.2628-2647.

[7]. Nandi, S., Mostakim, S.K. and Biswas, S., 2020. Rapid switch-on fluorescent detection of nanomolar-level hydrazine in water by a diacetoxy-functionalized MOF: application in paper strips and environmental samples. Dalton Transactions, 49(36), pp.12565-12573.

[8]. Kleist, W., Maciejewski, M. and Baiker, A., 2010. MOF-5 based mixed-linker metal–organic frameworks: Synthesis, thermal stability and catalytic application. Thermochimica Acta, 499(1-2), pp.71-78.

[9]. Song, Y.F. and Cronin, L., 2008. Postsynthetic covalent modification of metal–organic framework (MOF) materials. Angewandte Chemie International Edition, 47(25), pp.4635-4637.

[10]. Lian, X., Fang, Y., Joseph, E., Wang, Q., Li, J., Banerjee, S., Lollar, C., Wang, X. and Zhou, H.C., 2017. Enzyme–MOF (metal–organic framework) composites. Chemical Society Reviews, 46(11), pp.3386-3401.

[11]. Ikigaki, K., Okada, K., Tokudome, Y., Toyao, T., Falcaro, P., Doonan, C.J. and Takahashi, M., 2019. MOF-on-MOF: Oriented Growth of Multiple Layered Thin Films of Metal–Organic Frameworks. Angewandte Chemie, 131(21), pp.6960-6964.

[12]. Stock, N. and Biswas, S., 2012. Synthesis of metal-organic frameworks (MOFs): routes to various MOF topologies, morphologies, and composites. Chemical reviews, 112(2), pp.933-969.

[13]. Zhu, X., Zheng, H., Wei, X., Lin, Z., Guo, L., Qiu, B. and Chen, G., 2013. Metal–organic framework (MOF): a novel sensing platform for biomolecules. Chemical Communications, 49(13), pp.1276-1278.

[14]. Masoomi, M.Y., Morsali, A., Dhakshinamoorthy, A. and Garcia, H., 2019. Mixed-metal MOFs: unique opportunities in metal–organic framework (MOF) functionality and design. Angewandte Chemie, 131(43), pp.15330-15347.

[15]. Chen, J., Zhang, B., Qi, L., Pei, Y., Nie, R., Heintz, P., Luan, X., Bao, Z., Yang, Q., Ren, Q. and Zhang, Z., 2020. Facile fabrication of hierarchical MOF–Metal nanoparticle tandem catalysts for the synthesis of bioactive molecules. ACS Applied Materials & Interfaces, 12(20), pp.23002-23009.

[16]. Allmond, K., Stone, J., Harp, S. and Mujibur, K., 2017. Synthesis and electrospraying of nanoscale MOF (metal organic framework) for high-performance CO2 adsorption membrane. Nanoscale Research Letters, 12(1), pp.1-12.

[17]. Mueller, U., Schubert, M., Teich, F., Puetter, H., Schierle-Arndt, K. and Pastre, J., 2006. Metal–organic frameworks—prospective industrial applications. Journal of Materials Chemistry, 16(7), pp.626-636.

[18]. Kim, K.J., Li, Y.J., Kreider, P.B., Chang, C.H., Wannenmacher, N., Thallapally, P.K. and Ahn, H.G., 2013. High-rate synthesis of Cu–BTC metal–organic frameworks. Chemical Communications, 49(98), pp.11518-11520.

[19]. Ren, J., Dyosiba, X., Musyoka, N.M., Langmi, H.W., Mathe, M. and Liao, S., 2017. Review on the current practices and efforts towards pilot-scale production of metal-organic frameworks (MOFs). Coordination Chemistry Reviews, 352, pp.187-219.